Clin. Lab. 2026;72:XXX-XXX
©Copyright

ORIGINAL ARTICLE

A SenMayo-Related lncRNA Signature Predicts Prognosis and Reveals Molecular Characteristics in Hepatocellular Carcinoma

Haixia Li [1], Li Cao [2], Jianjun Gao [2], Ruimin Li [2], Xiaoqiang Lian [2], Xiaona Wei [1]

[1] *Department of Anesthesiology, Handan Central Hospital, Handan, China*
[2] *Department of Clinical Laboratory, Handan Central Hospital, Handan, China*

ABSTRACT

Background: **Cellular senescence and long non-coding RNAs (lncRNAs) have been demonstrated to play complex roles in the tumorigenesis and progression of hepatocellular carcinoma (HCC). This study aimed to establish a senescence-related lncRNA signature for predicting the prognosis of HCC patients and to identify potential biomarkers and therapeutic targets.**

Methods: **High-throughput sequencing and clinical data for HCC were obtained from The Cancer Genome Atlas (TCGA). A total of 125 SenMayo genes were compiled, and SenMayo-related lncRNAs (SM-lncRNAs) were identified using Pearson's correlation analysis. HCC patients were subsequently classified via consensus clustering, and Kaplan-Meier survival analysis was performed to evaluate differences between subgroups. An SM-lncRNA signature was constructed using LASSO-Cox regression, and its prognostic performance was assessed through Kaplan-Meier analysis and receiver operating characteristic (ROC) curves. Furthermore, differences in biological pathway enrichment, immune-related functions, and somatic mutation profiles were compared between high- and low-risk groups. Finally, a nomogram was developed using Cox proportional hazards regression (RMS R package) to predict 1-, 3-, and 5-year overall survival in HCC patients.**

Results: **A total of 366 HCC patients were included from TCGA-LIHC. Pearson's correlation analysis identified 1,450 SM-lncRNAs (r > 0.4). LASSO-Cox regression further selected four SM-lncRNAs (TMCC1-AS1, AC0113-37.1, AC010996.1, and AC009005.1) to construct a risk model, with high-risk (HR) patients exhibiting significantly lower survival than low-risk (LR) patients. The model demonstrated robust predictive performance, with ROC AUCs of 0.78, 0.75, and 0.70 at 1, 3, and 5 years in the training set; 0.74, 0.69, and 0.60 in the validation set; and 0.76, 0.70, and 0.65 overall. Multivariate Cox analysis identified the risk score and AJCC stage as independent prognostic factors. The survival nomogram achieved an AUC of 0.82 for 1-year survival, with calibration curves confirming its predictive accuracy.**

Conclusions: **This study established a 4-SenMayo-related lncRNA prognostic signature for HCC, demonstrating strong predictive performance and independent prognostic value alongside AJCC stage. The corresponding nomogram (1-year AUC = 0.82) further improved prognostic accuracy, offering a novel tool for HCC risk stratification and potential guidance for biomarker discovery.**

(Clin. Lab. 2026;72:xx-xx. DOI: 10.7754/Clin.Lab.2025.251145)

Correspondence:
Xiaoqiang Lian
Department of Clinical Laboratory
Handan Central Hospital
No. 59 Congtai North Road
Handan City
China
Email: lalmail@126.com

Xiaona Wei
Department of Anesthesiology
Handan Central Hospital
No. 59 Congtai North Road
Handan City
China
Email: tzyzxmuhong@163.com

Manuscript accepted December 5, 2025

KEYWORDS

Hepatocellular carcinoma, cellular senescence, SenMayo genes, long non-coding RNA, nomogram

INTRODUCTION

Hepatocellular carcinoma (HCC) is the sixth most common cancer and the third leading cause of cancer-related death worldwide [1], with over 50% of global HCC-related deaths occurring in China. Despite substantial advances in HCC treatment, patients continue to experience high post-surgical recurrence and low overall survival, largely due to the lack of accurate diagnostic and prognostic biomarkers.

Cellular senescence, defined as the permanent cessation of the cell proliferation cycle, plays a central role in organismal aging and disease progression, including embryogenesis, tissue remodeling, diabetes, and cancer [2]. The relationship between senescence and cancer is complex. On the one hand, senescent cells lose proliferative capacity, thereby inactivating and ultimately eliminating diseased or defective cells [3]; on the other hand, they secrete a variety of factors through the senescence-associated secretory phenotype (SASP). SASP components can disrupt the extracellular matrix and promote tumor invasion and metastasis by elevating local levels of cytokines, chemokines, matrix metalloproteinases, and other proteins [4,5]. Collectively, these findings indicate that cellular senescence is closely linked to tumor initiation and progression. Recently, a novel senescence gene set, SenMayo, has been developed. This gene set identifies cells with high expression of senescence/SASP genes and overcomes the limitations of transcription-based senescent cell detection at the single-cell level [6].

Emerging evidence highlights that senescence-related long non-coding RNAs (lncRNAs) play pivotal roles in the direct or indirect regulation of oncogenes [3]. For instance, lncRNA HEIH inhibits ovarian cancer cell senescence via the miR-3619-5p/CTTNB1P2 axis [7]; lncRNA MIAT suppresses breast cancer cell senescence by modulating p53 activity [8]; lncRNA PINT87aa induces HCC cell senescence through inhibition of FOXM1-mediated PHB2 [9]; and lncRNA H19 has been identified as a key regulator of cellular senescence and prostate cancer-related pathways [10]. These studies underscore the critical role of senescence-related lncRNAs in tumorigenesis and suggest their potential as biomarkers or therapeutic targets in cancer. Accordingly, this study aimed to develop a novel senescence-associated lncRNA model for predicting prognosis in HCC patients.

MATERIALS AND METHODS

Data acquisition and identification of SenMayo-related lncRNAs (SM-lncRNAs)

High-throughput sequencing data and clinical information for HCC patients were obtained from The Cancer Genome Atlas (TCGA), including gender, age, AJCC stage, tumor grade, survival time, and survival status. A total of 125 SenMayo genes were retrieved from a previously published study by Dominik Saul et al [6]. Differentially expressed genes (DEGs) between HCC and normal tissues were identified using the limma R package, with $|\log FC| > 1$ and $p < 0.05$ considered statistically significant.

Pearson's correlation analysis was performed between the differentially expressed SenMayo genes and lncRNAs. LncRNAs with a correlation coefficient > 0.4 and $p < 0.0001$ in relation to SenMayo genes were defined as SenMayo-related lncRNAs (SM-lncRNAs). Based on SM-lncRNA expression profiles, consensus clustering analysis was conducted to stratify HCC patients into distinct subgroups. Kaplan-Meier survival analysis was subsequently performed to evaluate differences in overall survival among these subgroups.

Construction and validation of a four-SM-lncRNA prognostic signature in HCC

HCC patients were randomly divided into training and validation sets at a 1:1 ratio using the caret R package. To reduce the dimensionality of SM-lncRNA variables, LASSO-Cox regression was performed on the training set. The risk score for each patient was calculated based on the expression levels of candidate SM-lncRNAs and their corresponding coefficients in the optimal model (determined by λ_minute).

Patients in both the training and validation cohorts were stratified into high-risk (HR) and low-risk (LR) groups according to the median risk score of the training set. Survival differences between the two groups were assessed using Kaplan-Meier analysis, and the predictive performance of the SM-lncRNA signature was evaluated with receiver operating characteristic (ROC) curves.

Clinical relevance of the SM-lncRNA prognostic signature

To investigate the relationship between the SM-lncRNA signature and clinical features in HCC patients, pre-calculated risk scores were used to stratify patients into high-risk and low-risk groups. These groups were further analyzed according to key clinical characteristics, including age, gender, tumor grade, and AJCC stage (Stage I vs. Stage II vs. Stage III–IV).

Transcriptomic, mutational, and immune profiling of high- and low-risk HCC patients

DEGs between HR and LR groups in the training set were identified using the limma R package, with $|\log FC| > 1$ and $p < 0.05$ considered statistically significant.

Functional enrichment analyses, including Gene Ontology (GO) biological process analysis and Kyoto Encyclopedia of Genes and Genomes (KEGG) pathway analysis, were performed using the clusterProfiler R package to explore the biological functions and pathways associated with these DEGs. To validate the enrichment results, Gene Set Variation Analysis (GSVA) was conducted using the GSVA R package.

Somatic mutation data of HCC patients from TCGA were stratified into HR and LR groups according to the SM-lncRNA signature. Mutation types and frequencies of key genes were summarized, and differences in mutational patterns between the two groups were compared.

To assess the immune landscape, the CIBERSORT algorithm was applied to RNA-seq data to estimate the relative proportions of immune cell subsets in HR and LR groups, and differences in immune cell infiltration were analyzed. Additionally, the ESTIMATE algorithm was used to calculate stromal, immune, and ESTIMATE scores for each patient, and differences between HR and LR groups were compared to evaluate consistency with CIBERSORT-derived immune infiltration results.

Integrated nomogram for individualized survival prediction in HCC

Cox proportional hazards regression was used to evaluate the prognostic significance of the SM-lncRNA risk score and clinical variables. A nomogram was constructed with the rms R package to predict 1-, 3-, and 5-year overall survival, integrating individual factor scores into a total score to estimate patient-specific survival probabilities. Nomogram performance was assessed via calibration curves and the concordance index (C-index).

RESULTS

Identification and clustering of SenMayo-related lncRNAs in HCC

A total of 366 HCC patients were included from the TCGA-LIHC cohort. Differential expression analysis of 125 SenMayo genes identified 50 genes with significant expression changes between tumor and adjacent normal tissues ($|\log_2 FC| > 1$, $p < 0.05$), comprising 15 upregulated and 35 downregulated genes (Figure 1A). Pearson's correlation analysis revealed 1,450 SenMayo-related lncRNAs (SM-lncRNAs) with a correlation coefficient $r > 0.4$ (Figure 1B). Consensus clustering based on SM-lncRNA expression stratified the 366 patients into two distinct subgroups (Figure 1C), and Kaplan-Meier survival analysis demonstrated significant differences in overall survival between these subgroups ($p = 0.039$; Figure 1D).

Construction and validation of a four-SM-lncRNA prognostic signature in HCC

HCC patients were randomly divided into training and validation cohorts at a 1:1 ratio. LASSO-Cox regression analysis in the training set identified four SM-lncRNAs (AC009005.1, TMCC1-AS1, AC011337.1, and AC010996.1) to construct the risk model (Figure 2A), with the risk score calculated as follows: Risk score = (AC009005.1 × 0.1046) + (TMCC1-AS1 × 0.5838) + (AC011337.1 × 0.0821) + (AC010996.1 × 0.6876).

Patients were stratified into HR and LR groups based on the median risk score of the training set. Heatmap analysis demonstrated a positive correlation between the expression of these four SM-lncRNAs and the risk score (Figure 2B). Kaplan–Meier survival analysis (Figure 2C) revealed significantly poorer overall survival in the HR group compared with the LR group across the training set ($p = 0.00089$), validation set ($p = 0.013$), and the combined cohort ($p < 0.0001$). ROC curves indicated robust predictive performance for 1-, 3-, and 5-year survival, with AUCs of 0.78, 0.75, and 0.70 in the training set; 0.74, 0.69, and 0.60 in the validation set; and 0.76, 0.70, and 0.65 in the overall cohort (Figure 2D).

Clinical relevance of the SM-lncRNA prognostic signature

To explore the relationship between the SM-lncRNA signature and clinical characteristics of HCC, risk scores were compared across different patient subgroups (Figure 3A - 3B). No significant differences in risk scores were observed with respect to gender (training set: $p = 0.029$; validation set: $p = 0.9$) or age (training set: $p = 0.91$; validation set: $p = 0.08$). In contrast, clear associations were observed for tumor grade and AJCC stage. Patients with high-grade tumors (G3+G4) exhibited significantly higher risk scores than those with low-grade tumors (G1+G2) (training set: $p = 0.00097$; validation set: $p = 7.3 \times 10^{-7}$). Similarly, patients with advanced AJCC stage (III+IV) showed markedly higher risk scores compared with Stage I patients (training set: $p = 0.00088$; validation set: $p = 0.0083$).

Transcriptomic, mutational, and immune profiling of high- and low-risk HCC patients

Between the high-risk (HR) and low-risk (LR) groups, 328 genes were upregulated and 344 genes were downregulated ($|\log FC| > 1$, $p < 0.05$). GO enrichment analysis revealed that these DEGs were primarily associated with nuclear division, chromosome segregation, and related processes (Figure 4A). KEGG pathway analysis highlighted enrichment in the cell cycle (hsa04110) and oocyte meiosis (hsa04114) pathways (Figure 4B). GSVA further demonstrated elevated activities of double-strand break repair, C-5 methylation, and DNA replication in HR tissues (Figure 4C).

Figure 5 presents the somatic mutation landscape of HCC patients. Core genes such as TP53, CTNNB1, and TTN were frequently mutated (Figure 5A), predomi-

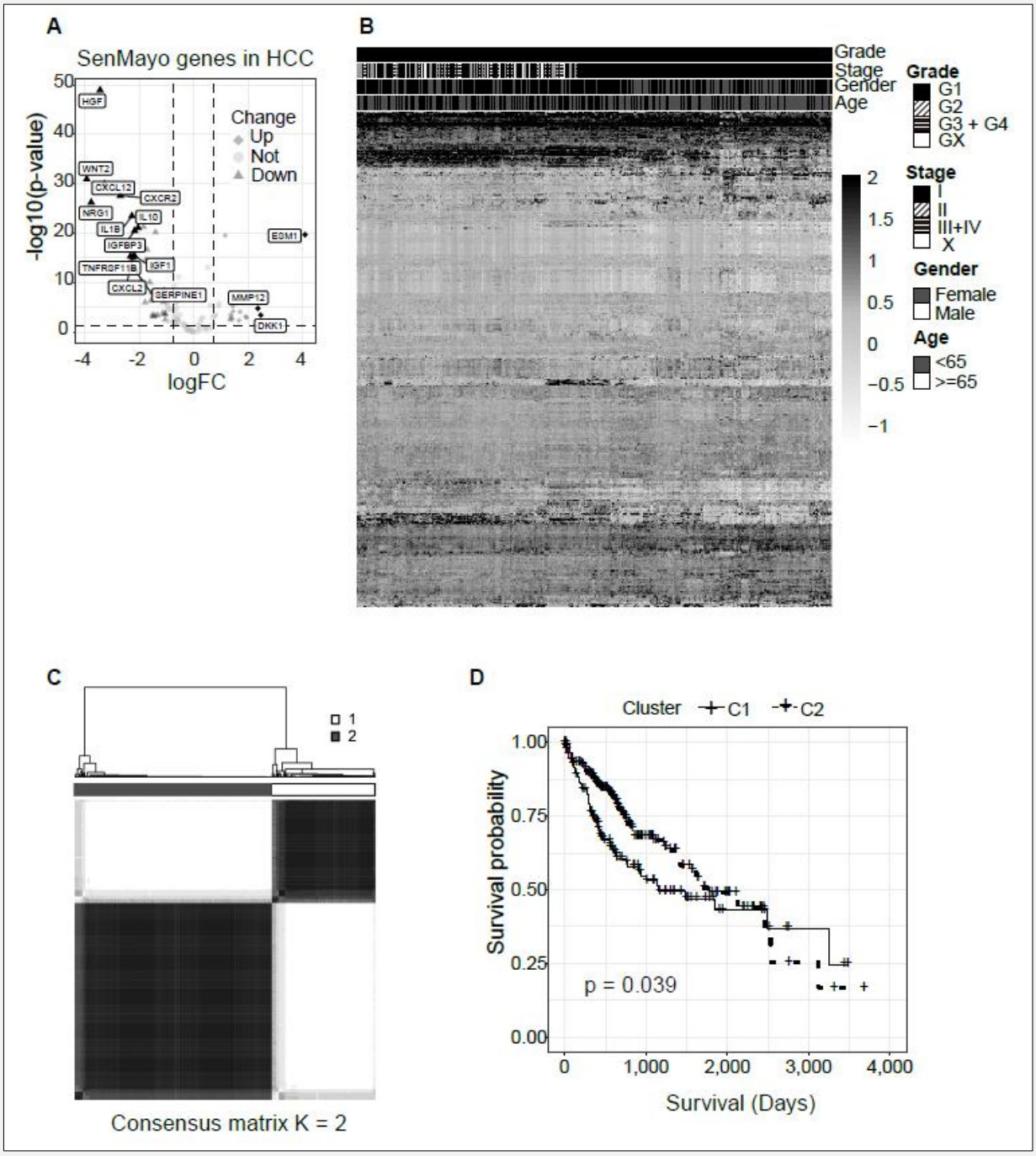


Figure 1. Characterization of SenMayo-related lncRNAs (SM-lncRNAs).

A: Differential expression analysis of 125 SenMayo genes in patients with HCC. B: Expression landscape of SM-lncRNAs in HCC. C: Consensus clustering of HCC patients based on SM-lncRNA expression profiles. D: Kaplan-Meier survival analysis of SM-lncRNA defined subtypes in the HCC cohort.

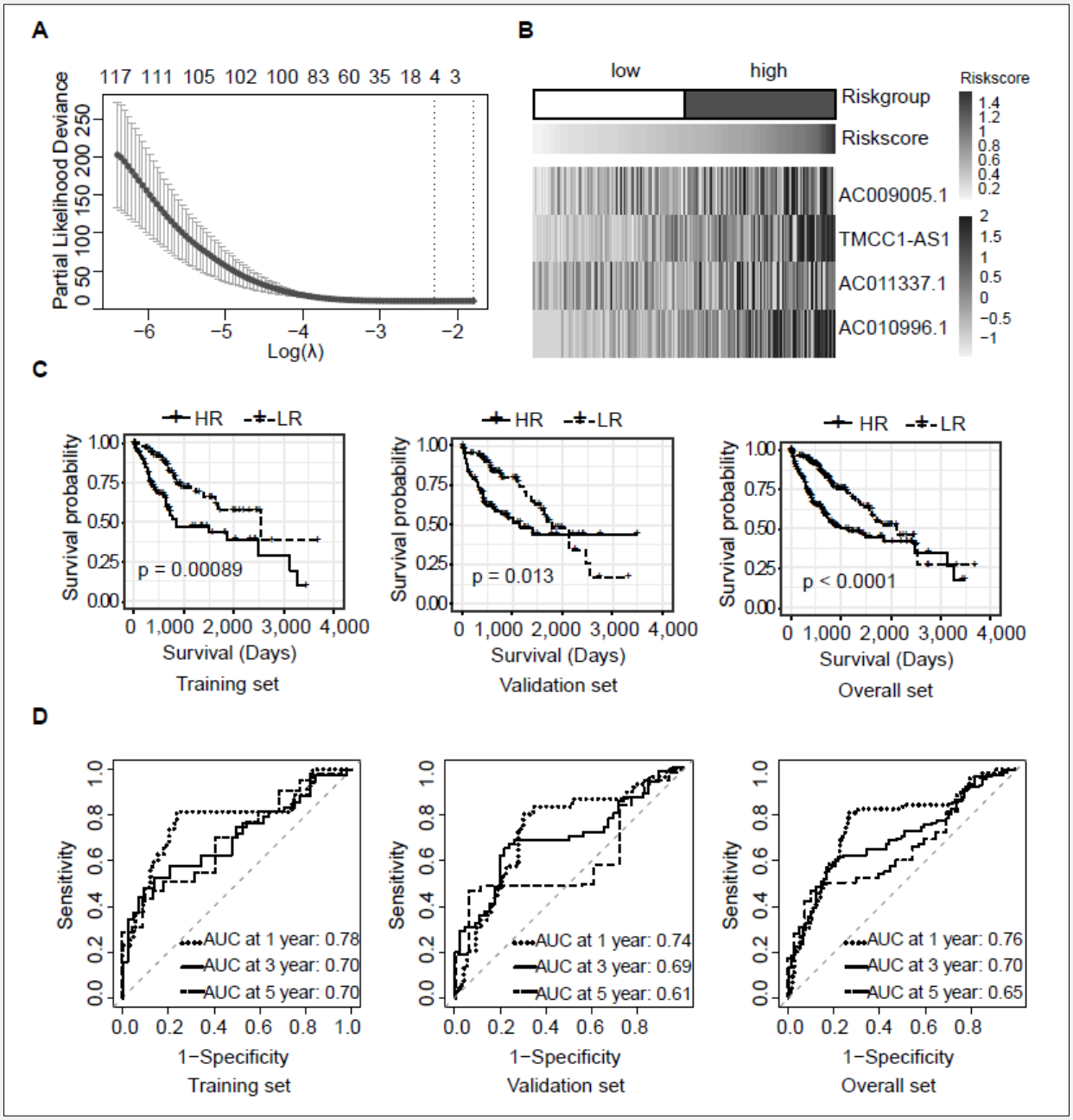


Figure 2. SM-lncRNA risk signature for predicting HCC prognosis.

A: LASSO-Cox regression analysis of SM-lncRNAs. B: Distribution of SM-lncRNA-based risk scores across HCC subgroups. C: Kaplan-Meier survival curves comparing high- and low-risk groups in the training, validation, and overall sets. D: ROC curves for 1-, 3-, and 5-year overall survival prediction in the training, validation, and overall sets.

nantly via missense mutations, in the training set (Figures 5B). Notably, mutation patterns differed between HR and LR subgroups, with TP53 mutations significantly enriched in the HR group across the training set (Figure 5C).

CIBERSORT analysis indicated that macrophages were the most abundant immune cell population in HCC, followed by T cells (Figure 6A), with no significant differences in immune cell proportions between HR and LR groups in the training set (Figure 6B). ESTIMATE anal-

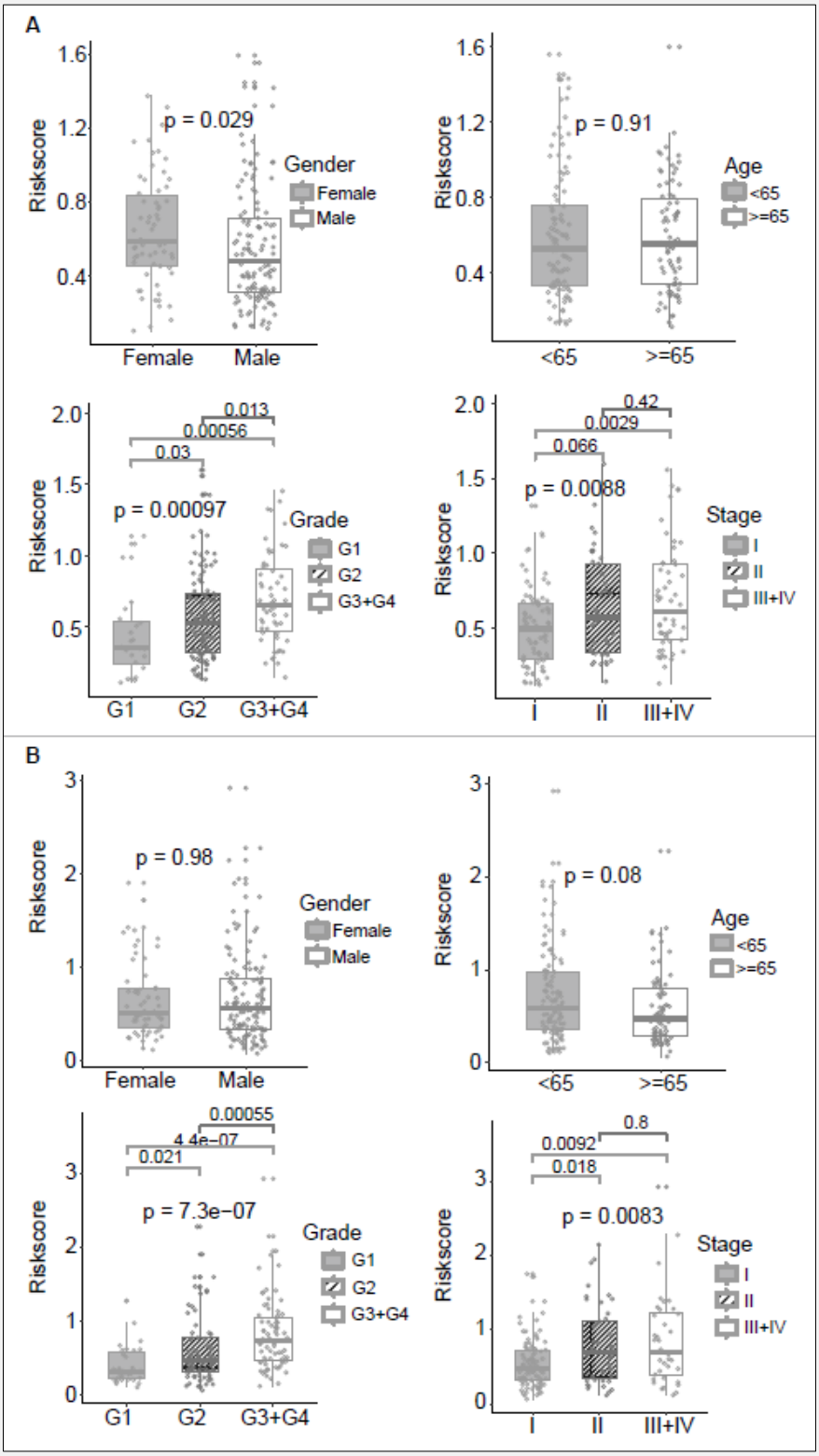


Figure 3. Association between the risk score and clinical characteristics.

A, B: Boxplots with jitter showing the distribution of risk scores across gender, age, tumor grade, and pathological stage in the training (A) and validation (B) sets.

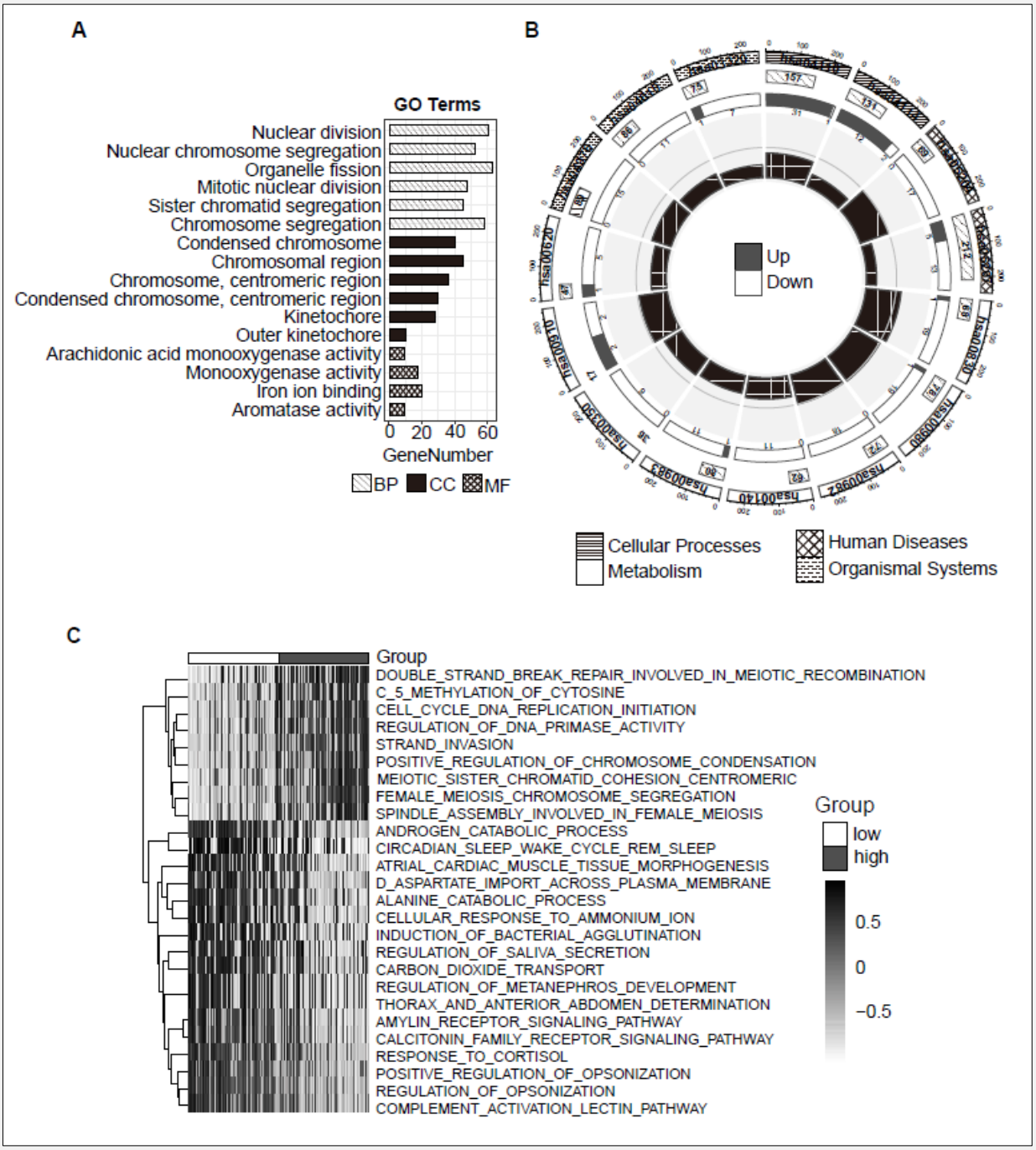


Figure 4. Biological function profiling between risk subgroups in the training set.

A, B: GO (A) and KEGG (B) pathway enrichment analyses of differentially expressed genes between high- and low-risk groups. C: GSVA-based functional enrichment analysis comparing pathway activity between high- and low-risk groups.

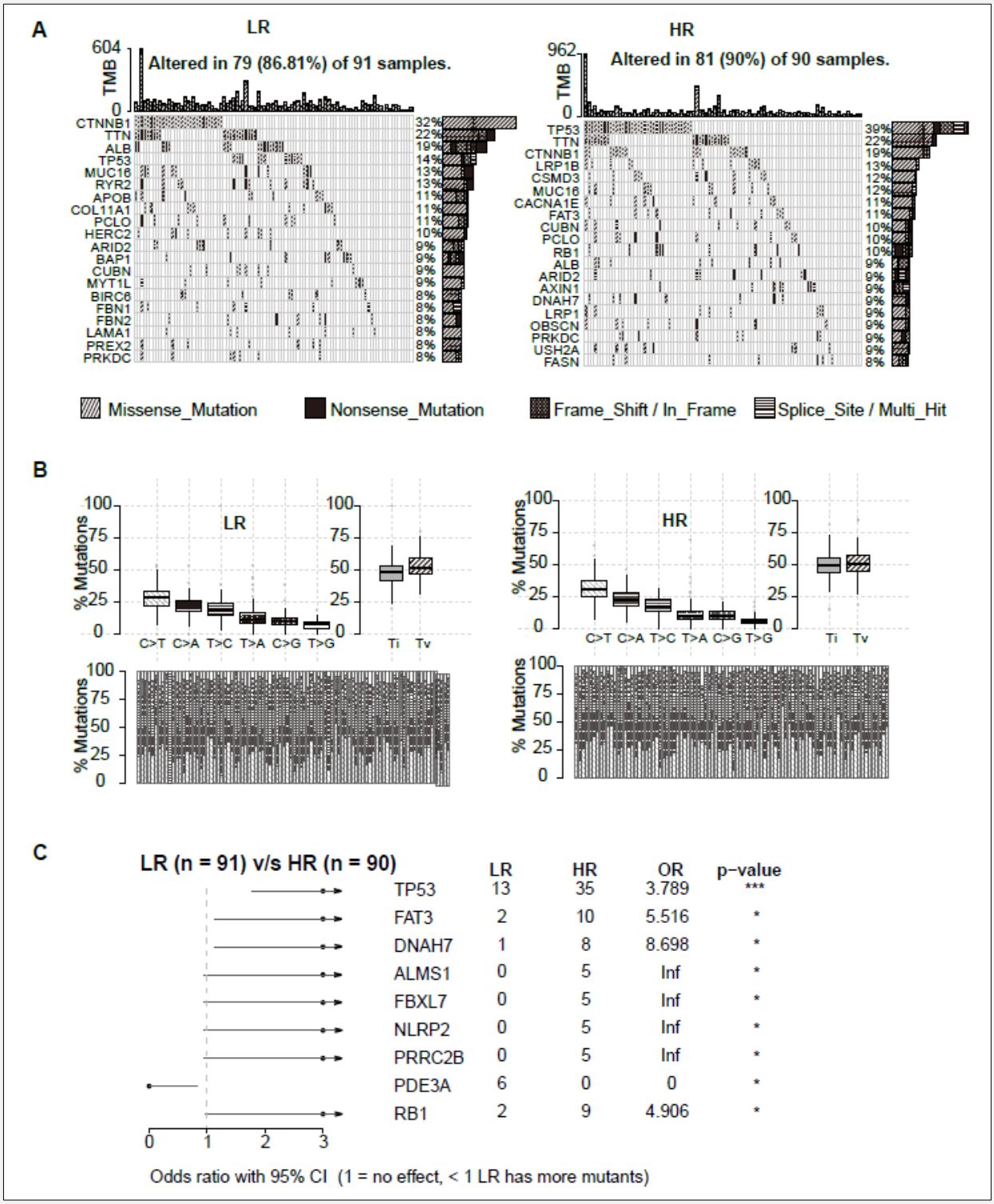


Figure 5. Somatic mutation profiles across risk subgroups.

A: Somatic mutation landscapes of the HR and LR subgroups in the training set. The top bars indicate sample-level tumor mutation burden (TMB), and the side bars represent the number of samples harboring each mutation. B: Proportion of mutation types of risk subgroups in training set. C: Differential mutation analysis between risk subgroups in the training set. (* $p < 0.05$; ** $p < 0.01$; *** $p < 0.001$).

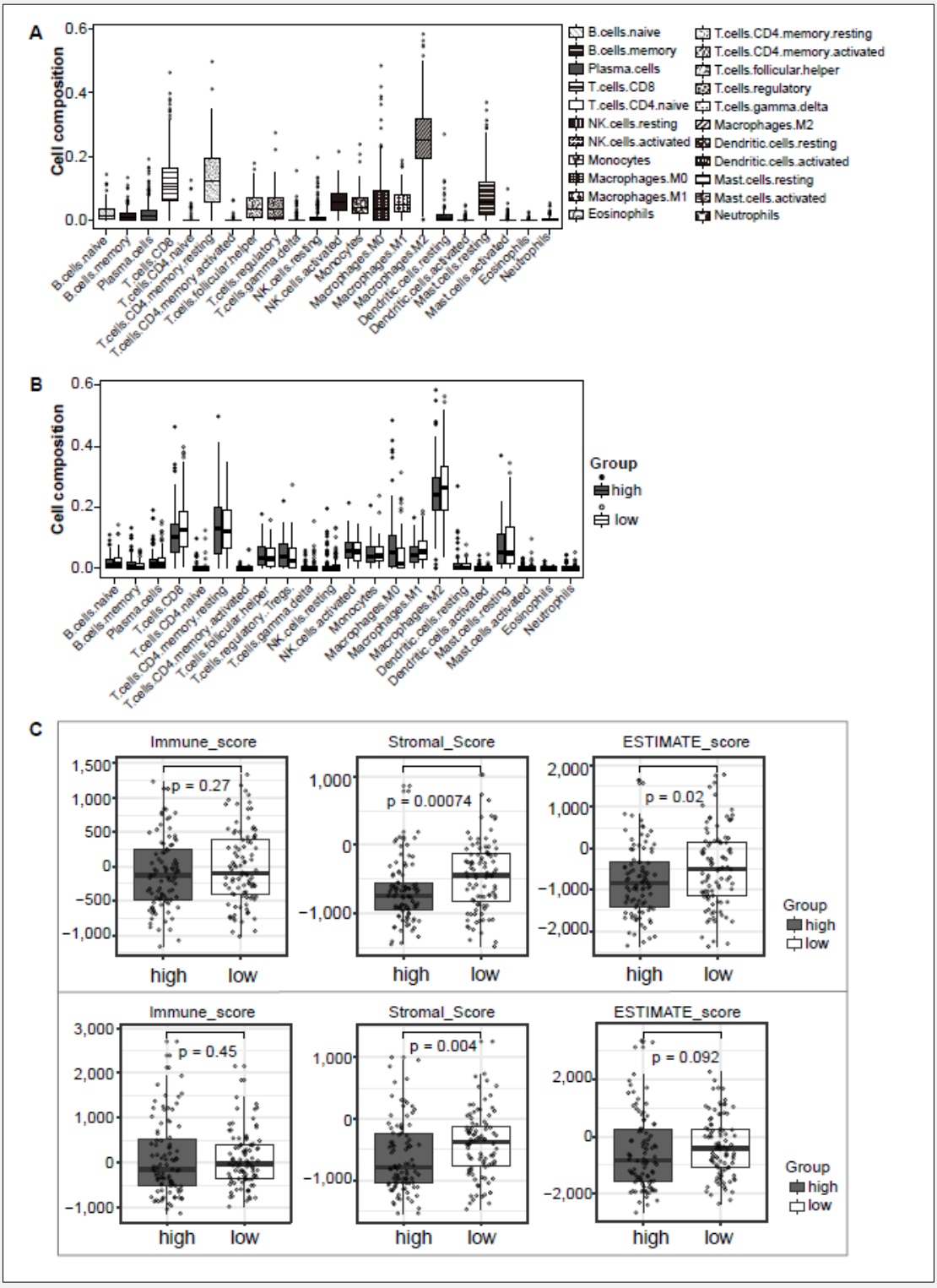


Figure 6. Tumor microenvironment profiles across risk subgroups.

A: Relative abundances of 20 immune cell types estimated using the CIBERSORT algorithm in the training set. B: The proportions of infiltrating immune cells did not differ significantly between the HR and LR subgroups in the training cohort. C: Stromal, immune, and overall ESTIMATE scores of HCC tissues (upper panel: training cohort; lower panel: validation cohort) calculated using the ESTIMATE algorithm.

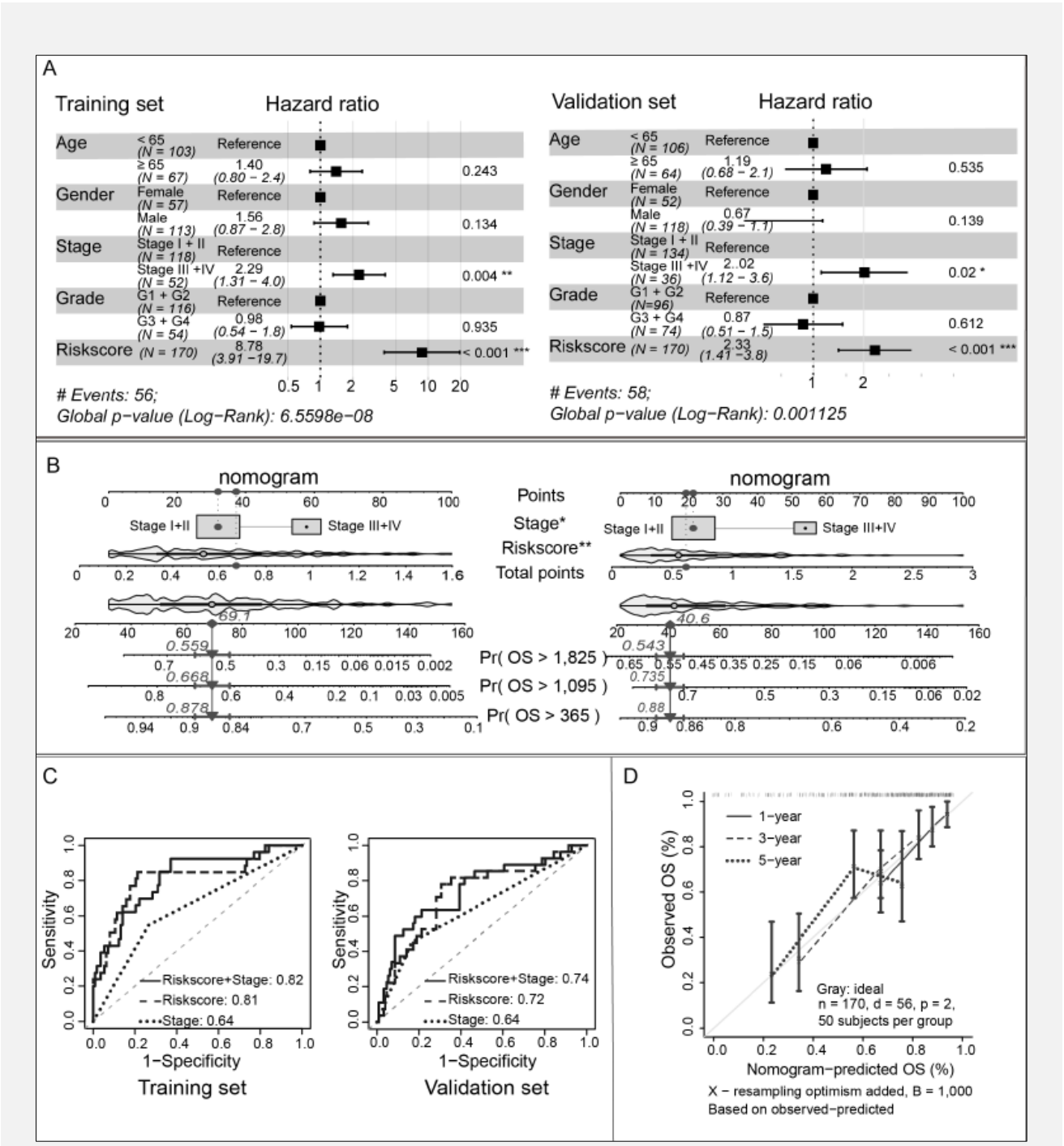


Figure 7. Construction and performance evaluation of the prognostic nomogram.

A: Forest plots of the multivariate Cox regression analysis (age, gender, stage, grade, and risk score) in the training and validation sets. B: Nomograms predicting 1-, 3-, and 5-year OS based on stage and risk score in the training and validation sets. C: ROC curves of the nomogram in the training and validation sets. D: Calibration curves of the nomogram in the training set.

ysis (Figure 6C) showed that HR tumors had lower stromal and overall ESTIMATE scores, indicating higher tumor purity, while immune scores were similar between the HR and LR groups, consistent with the CIBERSORT results. Collectively, these results suggest that HCC risk is more closely associated with tumor purity rather than differences in immune cell infiltration.

Integrated nomogram for individualized survival prediction in HCC

Multivariate Cox regression analysis revealed that the SM-lncRNA risk score and AJCC stage were independent prognostic factors for HCC in both the training and validation cohorts (Figure 7A). A nomogram integrating these two variables was developed to predict 1-, 3-, and 5-year overall survival (Figure 7B). The nomogram demonstrated strong predictive performance, with 1-year AUCs of 0.82 in the training set and 0.74 in the validation set, outperforming models based on risk score or AJCC stage alone (Figure 7C). Calibration curves for 1-, 3-, and 5-year survival showed excellent agreement between predicted and observed outcomes (Figure 7D). Collectively, these findings indicate that the integrated nomogram provides a reliable tool for individualized prognosis prediction in HCC patients.

DISCUSSION

HCC remains a major health burden due to its high morbidity and mortality. The development of novel, precise predictive biomarkers or models is essential for improving patient prognosis. In this study, we established a senescence-related lncRNA (SM-lncRNA) prognostic model using TCGA data, comprising four SM-lncRNAs significantly associated with HCC initiation and progression. We further developed a nomogram integrating the risk score and AJCC stage - both identified as independent prognostic factors - to provide a visual tool for individualized outcome prediction. Additionally, somatic mutations were correlated with poor prognosis, whereas no significant association was observed between immune cell infiltration and patient outcomes in this cohort. Collectively, these findings highlight the potential of combining molecular biomarkers with clinical variables to enhance the accuracy of prognostic models in HCC.

Emerging evidence highlights the pivotal role of long non-coding RNAs (lncRNAs) in tumorigenesis and cancer progression [11-13]. By interacting with DNA, RNA, or proteins - or even encoding small peptides - lncRNAs regulate key cellular processes, including proliferation, apoptosis evasion, angiogenesis, and acquisition of invasive potential [14]. Integrative analyses of multiple datasets identified 74 dysregulated lncRNAs in hepatocellular carcinoma (HCC) and clarified their mechanistic roles in hepatocarcinogenesis [15]. For example, Xu et al. reported that AK001796 promotes HCC cell proliferation by enhancing phospho-ERK1/2 and AKT signaling through the miR-150/GAB1 axis [16], whereas LINC02428 functions as a tumor suppressor by disrupting the KDM5B/IGF2BP1 positive feedback loop implicated in HCC development [17]. In parallel, cellular senescence, particularly via the senescence-associated secretory phenotype (SASP) that releases cytokines and growth factors, also contributes to tumor initiation and progression [18,19]. Collectively, these findings underscore the intricate interplay among lncRNAs, cellular senescence, and HCC pathogenesis. Recently, several studies have developed risk signatures to predict HCC prognosis based on transcriptomic profiles of senescence-related genes [3,4,20]. In contrast to these prior efforts, we employed a novel and previously unreported senescence gene set, SenMayo [6]. In this study, 125 SenMayo genes were retrieved from a published dataset by Dominik Saul et al., and a total of 1,450 senescence-associated prognostic lncRNAs were analyzed using data from The Cancer Genome Atlas (TCGA). Based on these analyses, a prognostic signature was constructed, and its predictive accuracy in HCC patients was evaluated using Kaplan-Meier survival curves and receiver operating characteristic (ROC) analyses. Four senescence-associated lncRNAs (SM-lncRNAs) - TMCC1-AS1, AC009005.1, AC010996.1, and AC011337.1 - were identified. Previous studies have reported that TMCC1-AS1 is upregulated in HCC, promoting cell proliferation, migration, invasion, and epithelial-to-mesenchymal transition [21], and its high expression correlates with advanced TNM stage, lymph node metastasis, and poorer survival [22]. LncRNA AC009005.1 has been shown to regulate autophagy pathways, influencing HCC initiation and progression [23]. In contrast, AC010996.1 - previously identified as an independent prognostic factor in cervical cancer [24] - and AC011337.1 have not yet been studied in HCC and warrant further investigation.

Senescent cells profoundly influence the tumor immune microenvironment, thereby promoting tumor growth and progression [25]. This observation prompted us to further investigate the impact of cellular senescence on the immune microenvironment of HCC. Our analysis revealed that macrophages and T cells constitute the predominant immune cell populations within the HCC microenvironment; however, no significant differences in immune cell infiltration were observed between the high- and low-risk groups. These findings were further corroborated using the ESTIMATE algorithm.

Notably, HCC patients often harbor mutations in genes such as TP53, CTNNB1, and TTN. We observed distinct somatic mutation profiles between the high- and low-risk subgroups, with TP53 mutations being significantly more frequent in the high-risk subgroup. Functional enrichment analyses, including GO, KEGG, and GSVA, indicated that these mutated genes are primarily involved in cell cycle regulation and DNA replication processes. As a key tumor suppressor, TP53 mutations allow cells to evade apoptosis and undergo malignant transformation following DNA damage, representing

the most common genetic alteration in HCC [26]. Consistent with previous reports [27,28], HCC patients harboring TP53 mutations tend to have shorter overall survival, aligning with our observation that high-risk subgroup patients exhibit poor prognosis.

Finally, we constructed a comprehensive predictive model integrating multiple factors, including risk score, age, and tumor stage, using multivariate Cox regression analysis. The results indicated that both risk score and tumor stage serve as independent prognostic factors for HCC. Calibration curves further confirmed that the model's predicted 1-, 2-, and 3-year survival probabilities closely matched the observed outcomes. These findings suggest that combining SM-lncRNA-based risk scores with tumor stage provides a robust tool for accurately predicting HCC prognosis, with predictive performance superior to that of individual variables alone.

In conclusion, we developed a cellular senescence-associated lncRNA predictive model for HCC based on gene expression profiles. This model demonstrates superior prognostic value compared to individual lncRNA markers and may serve as a valuable tool to guide clinical decision-making and enhance patient management. Nevertheless, our study has certain limitations. The predictive model was constructed solely using gene expression and clinical data from publicly available databases; therefore, further validation with independent clinical cohorts is necessary to assess its applicability across more diverse patient populations.

Declaration of Generative AI in Scientific Writing:
Generative AI tools were occasionally used to improve language clarity; all scientific content and analysis were performed by the authors.

Declaration of Interest:
No conflicts of interest declared.

References:

1. Bray F, Laversanne M, Sung H, et al. Global cancer statistics 2022: GLOBOCAN estimates of incidence and mortality worldwide for 36 cancers in 185 countries. CA Cancer J Clin 2024 May-Jun;74(3):229-63. (PMID: 38572751)

2. Calcinotto A, Kohli J, Zagato E, Pellegrini L, Demaria M, Alimonti A. Cellular Senescence: Aging, Cancer, and Injury. Physiol Rev 2019 Apr 1;99(2):1047-78. (PMID: 30648461)

3. Huang E, Ma T, Zhou J, et al. The development and validation of a novel senescence-related long-chain non-coding RNA (lncRNA) signature that predicts prognosis and the tumor microenvironment of patients with hepatocellular carcinoma. Ann Transl Med 2022 Jul;10(14):766. (PMID: 35965795)

4. Gao C, Zhou G, Cheng M, Feng L, Cao P, Zhou G. Identification of senescence-associated long non-coding RNAs to predict prognosis and immune microenvironment in patients with hepatocellular carcinoma. Front Genet 2022 Oct 13;13:956094. (PMID: 36330438)

5. Kahlem P, Dörken B, Schmitt CA. Cellular senescence in cancer treatment: friend or foe? J Clin Invest 2004 Jan;113(2):169-74. (PMID: 14722606)

6. Saul D, Kosinsky RL, Atkinson EJ, et al. A new gene set identifies senescent cells and predicts senescence-associated pathways across tissues. Nat Commun 2022 Aug 16;13(1):4827. (PMID: 35974106)

7. Si L, Chen J, Yang S, et al. lncRNA HEIH accelerates cell proliferation and inhibits cell senescence by targeting miR-3619-5p/CTTNBP2 axis in ovarian cancer. Menopause 2020 Nov;27(11):1302-14. (PMID: 33110047)

8. Alipoor FJ, Asadi MH, Torkzadeh-Mahani M. MIAT lncRNA is overexpressed in breast cancer and its inhibition triggers senescence and G1 arrest in MCF7 cell line. J Cell Biochem 2018 Aug;119(8):6470-81. (PMID: 29345338)

9. Xiang X, Fu Y, Zhao K, et al. Cellular senescence in hepatocellular carcinoma induced by a long non-coding RNA-encoded peptide PINT87aa by blocking FOXM1-mediated PHB2. Theranostics 2021 Mar 4;11(10):4929-44. (PMID: 33754036)

10. da Silveira WA, Renaud L, Hazard ES, Hardiman G. miRNA and lncRNA Expression Networks Modulate Cell Cycle and DNA Repair Inhibition in Senescent Prostate Cells. Genes (Basel) 2022 Jan 24;13(2):208. (PMID: 35205253)

11. Klingenberg M, Matsuda A, Diederichs S, Patel T. Non-coding RNA in hepatocellular carcinoma: Mechanisms, biomarkers and therapeutic targets. J Hepatol 2017 Sep;67(3):603-18. (PMID: 28438689)

12. He Y, Meng XM, Huang C, et al. Long noncoding RNAs: Novel insights into hepatocelluar carcinoma. Cancer Lett 2014 Mar 1;344(1):20-7. (PMID: 24183851)

13. Shi L, Wang Q, Lv J, Liu Q, Wu J. Differential Analysis of IncRNAs and mRNAs Expression in HCC and the Predictive Value of lncRNAs. J Environ Pathol Toxicol Oncol 2021;40(4):73-85. (PMID: 34936302)

14. Wang C, Vegna S, Jin H, et al. Inducing and exploiting vulnerabilities for the treatment of liver cancer. Nature 2019 Oct;574(7777):268-72. (PMID: 31578521)

15. Lim LJ, Wong SYS, Huang F, et al. Roles and Regulation of Long Noncoding RNAs in Hepatocellular Carcinoma. Cancer Res 2019 Oct 15;79(20):5131-9. (PMID: 31337653)

16. Xu R, He H, Wang Y, et al. LncRNA AK001796 promotes cell proliferation via acting as a ceRNA of miR-150 in hepatocellular carcinoma. Genet Mol Biol 2023 Jun 2;46(2):e20220277. (PMID: 37272834)

17. Du X, Zhou P, Zhang H, et al. Downregulated liver-elevated long intergenic noncoding RNA (LINC02428) is a tumor suppressor that blocks KDM5B/IGF2BP1 positive feedback loop in hepatocellular carcinoma. Cell Death Dis 2023 May 3;14(5):301. (PMID: 37137887)

18. Saul D, Kosinsky RL. Single-Cell Transcriptomics Reveals the Expression of Aging- and Senescence-Associated Genes in Distinct Cancer Cell Populations. Cells 2021 Nov 11;10(11):3126. (PMID: 34831349)

19. Yamagishi R, Kamachi F, Nakamura M, et al. Gasdermin D-mediated release of IL-33 from senescent hepatic stellate cells promotes obesity-associated hepatocellular carcinoma. Sci Immunol 2022 Jun 24;7(72):eabl7209. (PMID: 35749514)

20. Sun R, Wang X, Chen J, et al. Development and validation of a novel cellular senescence-related prognostic signature for predicting the survival and immune landscape in hepatocellular carcinoma. Front Genet 2022 Sep 6;13:949110. (PMID: 36147502)

21. Xu L, Chen S, Li Q, et al. Integrating bioinformatics and experimental validation to unveil disulfidptosis-related lncRNAs as prognostic biomarker and therapeutic target in hepatocellular carcinoma. Cancer Cell Int 2024 Jan 13;24(1):30. (PMID: 38218909)

22. Gao XF, Xu XL, Zhang JH, et al. A novel disulfidptosis-related lncRNAs index to predict prognosis and therapeutic target in hepatocellular carcinoma. Transl Cancer Res 2025 Oct 31;14(10): 7053-70. (PMID: 41234897)

23. Wu H, Liu T, Qi J, Qin C, Zhu Q. Four Autophagy-Related lncRNAs Predict the Prognosis of HCC through Coexpression and ceRNA Mechanism. Biomed Res Int 2020 Oct 9;2020: 3801748. (PMID: 33102579)

24. Lang X, Huang C, Cui H. Prognosis Analysis and Validation of Fatty Acid Metabolism-Related lncRNAs and Tumor Immune Microenvironment in Cervical Cancer. J Immunol Res 2022 Jul 28;2022:4954457. (PMID: 35942212)

25. Park SS, Choi YW, Kim JH, Kim HS, Park TJ. Senescent tumor cells: an overlooked adversary in the battle against cancer. Exp Mol Med 2021 Dec;53(12):1834-41. (PMID: 34916607)

26. Long J, Wang A, Bai Y, et al. Development and validation of a TP53-associated immune prognostic model for hepatocellular carcinoma. EBioMedicine 2019 Apr;42:363-74. (PMID: 30885723)

27. Liu J, Ma Q, Zhang M, et al. Alterations of TP53 are associated with a poor outcome for patients with hepatocellular carcinoma: evidence from a systematic review and meta-analysis. Eur J Cancer 2012 Oct;48(15):2328-38. (PMID: 22459764)

28. Yang C, Huang X, Li Y, Chen J, Lv Y, Dai S. Prognosis and personalized treatment prediction in TP53-mutant hepatocellular carcinoma: an in silico strategy towards precision oncology. Brief Bioinform 2021 May 20;22(3): bbaa164. (PMID: 32789496)